High Resolution PolInSAR with the Ground-Based SAR (GB-SAR) System: Measurement and Modelling

Keith Morrison
Dept. Of Aerospace, Power and Sensors,
University of Cranfield,
Swindon SN6 8LA, UK
k.morrison@cranfield.ac.uk

Mark L. Williams
IMES Group, DSTO,
PO Box 1500, Edinburgh,
SA 5111, AUSTRALIA
mark.williams@dsto.defence.gov.au

***Abstract* — Ground-based work is necessary for a comprehensive assessment of the operational potential and limitations of PolInSAR in airborne and satellite SAR applications. A study is made of the performance and usefulness of the UK's Ground-Based SAR (GB-SAR) Outdoor System in high-resolution PolInSAR studies of vegetation using modeling results. The facility provides fully-polarimetric L- through X-band imagery down to a resolution of several wavelengths. However, the measurement process is slow in relation to pulsed systems as it requires the antenna head to be mechanically scanned across an aperture. The PolInSAR technique requires high coherence between interferometric image pairs, and the long data acquisition times raise the question of temporal decorrelation. We developed two models incorporating motion, a physics-based model and a signal processing model. The former incorporates a PolInSAR crop simulator employing the distorted Born approximation, applied to a simulated canopy of wheat plants based on field-collected physiological measurements. GB-SAR simulations of mature wheat canopies suffering a range of wind-blown disturbances are examined for coherence stability. These calculations permit the analysis of the behaviour of coherence with system and canopy descriptive parameters, such to quantify the suitability and performance of measurement environments for PolInSAR analysis. The models indicate that clutter motion will degrade interferometric performance both during aperture formation, and between repeat-pass observation. However, we conclude that the GB-SAR system will be robust to small amounts of clutter motion and will serve as a suitable tool for PolInSAR experimental studies.**

I. Introduction

Over the past few years novel observing techniques have been developed exploiting fully polarimetric and interferometric capabilities of which polarimetric SAR interferometry (PolInSAR) is the most prominent [1]. It exploits the polarisation dependence of scattering mechanisms to estimate scattering phase centre heights, which can be extrapolated to retrieve plant height. However, no comprehensive assessment of the operational potential and limitations of PolInSAR are yet available. Particular open questions relate to the conditions under which PolInSAR produces accurate results, with respect to:

i) structural canopy types
ii) technical sensor specifications
iii) imaging conditions (spatial and temporal).

Figure 1. The deployed GB-SAR Outdoor System.

To help answer these questions, it is proposed to utilise the UK's Ground-Based SAR (GB-SAR) Outdoor System [2] in a campaign of well controlled and coordinated experiments on vegetation canopies. The deployed system is shown in Fig. 1. Currently, the portable system provides fully-polarimetric L-through X-band high-resolution SAR imagery, and is to be upgraded to provide the necessary interferometric capability. The RF sub-system is based around a stepped-frequency CW radar system, which provides great flexibility in the equivalent time-domain waveforms that can be realized. However, the measurement process is slow in relation to pulsed systems as the aperture is built up by the mechanical scanning of the polarimetric antenna head at ~$\lambda/4$ increments across the 4m aperture. At each measurement position, the response of the target to a series of discrete frequencies stepped over a prescribed bandwidth is measured. The total imaging time is dependent upon the radar frequency in use, but is of the order of several minutes. Polarimetric scans are built up by repeat scans with the appropriate antennas switched in.

The PolInSAR technique requires high coherence between interferometric image pairs, and the long data acquisition times raise the question of significant temporal decorrelation due to wind disturbance of the canopy. This paper analyses the significance of consequences of target motion with respect to the suitability of ground-based measurements for PolInSAR investigation.

II. Physics-Based SAR Image Simulation

A.. Coherent Modeling Strategy

As with any radar calculation we require a suitable description of the target. The techniques used to generate the model wheat canopy are described fully in [3]. Our wheat canopy consists of a distribution of wheat plants each modeled as a cluster of curved stems, with ears and leaves (curved and twisted strips) attached. We model a mature wheat canopy, post-heading with approximately 500 stems per square meter (Fig. 2). The model is based on field-collected physiological measurements [4,5,6,7].

The simulation is physics-based, using the distorted-Born approximation, and accounting for canopy inhomogeneity. The output of the simulation is simulated, coherent, fully polarimetric, single-look-complex SAR imagery, described in [3], and references therein.

B. Effects of Crop Motion on Coherence

During GB-SAR data acquisition crop motion influences the final coherence image in two ways: during aperture formation, and between aperture formation. The effects of scatterer motion during aperture formation are discussed in the following section. Here we consider the effects of inter-aperture displacements and assume, for the present, that intra-aperture displacements have little effect other than to broaden the point spread function.

Clutter motion has been modeled by varying the curvature of wheat stems. An increase in stem curvature corresponds to bending motion similar to that induced by wind pressure. The resulting displacements along the stem increase with height from zero at ground level to a maximum for ear tips. We have modeled two cases, one with small RMS ear tip displacements of 0.7cm, and the other with larger displacements of 1.3cm.

We have chosen to simulate at C-Band, with an antenna height of 10m, and ground-ranges of 10.0m, 10.1m, 10.2m and 10.3m yielding three baselines. We simulate an area some 6m by 6m at ~15cm resolution in ground-range and azimuth, and analyze a central area 4m by 4m in the resulting imagery, which is representative of a homogeneous canopy and clear of boundary effects resulting from layover. An example of simulated imagery and coherence images is provided in Fig. 3. Backscattering coefficients are reported in Table I and are useful in interpreting the results.

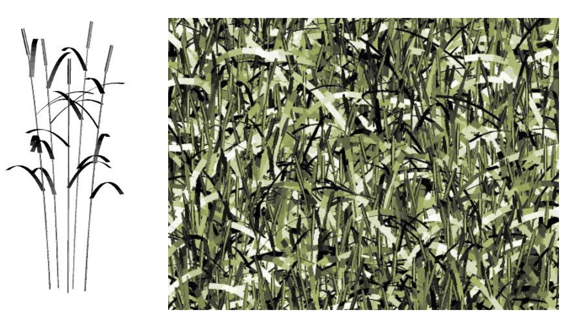

Figure 2. Example of model wheat plant and wheat canopy used in the SAR simulation.

TABLE I
SIMULATED WHEAT BACKSCATTERING COEFFICIENTS.

	HH (dB)	HV (dB)	VV (dB)
Direct Ground	-19.0	-58.2	-30.6
Direct Volume	-14.6	-33.0	-18.3
Ground Volume	-13.6	-27.7	-21.6
Total	**-10.4**	**-26.3**	**-16.6**

A full description of the polarimetric response of the data is to be found in [3]. We observe here that V attenuation is much greater than H in the canopy and as a result VV returns are predominantly from material at the top of the canopy. At the same time VV is darker than HH, and HV is somewhat under-estimated as a result of neglecting volume-volume interactions in the model. Nevertheless the results are in good agreement with observations [3]. We observe that whilst direct volume terms dominate the VV response, ground-volume terms are strongest in HH and most clearly seen in HV. Thus HV returns have phase centers close to the ground in this model, although they are weak and are likely to be in competition with noise and incoherent backscatter, which has not been modeled.

In Fig. 4 we report the results of direct-volume coherence calculations by polarimetric channel as a function of increasing baseline, with varying amounts of clutter displacement. With no clutter motion coherence is high and VV demonstrates the greatest coherence. This is in keeping with our observation that attenuation for V polarization is strong and most returns come from near the top of the canopy yielding a well-defined phase centre. Perversely, when the effects of clutter motion are incorporated into the calculation, VV coherence falls the most: motion at the top of the canopy is greatest and hence has the strongest effect on the coherence of the VV returns that originate there. This model is in keeping with recent X-Band observations for coherence over a wheat canopy of similar height [8]. We observe that for RMS wheat ear displacements of 1.3cm the model predicts that coherence in VV is all but lost, and this would then preclude the possibility of recovering crop height using interferometric techniques.

For smaller motion RMS displacements of 0.7cm volume

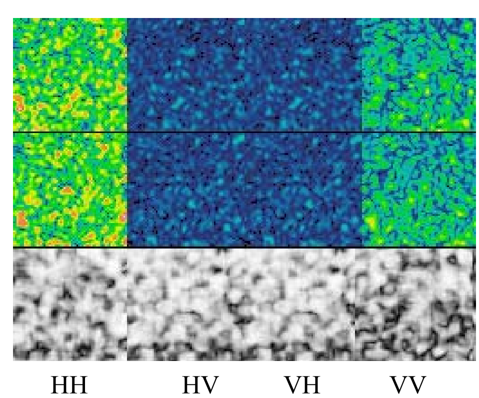

Figure 3. Simulated GB-SAR images of wheat for the 20cm baseline with no clutter motion and the resulting coherence image formed using a 5 by 5 window.

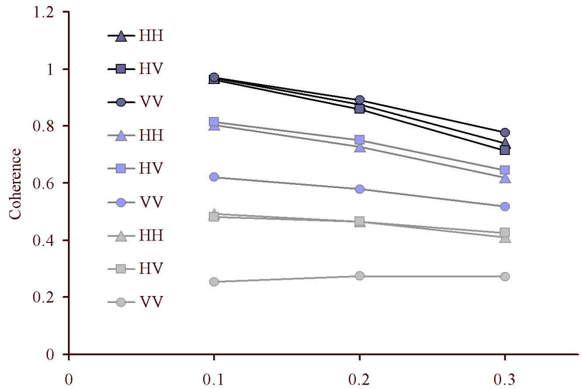

Fig 4. Effects of inter-aperture clutter motion on interferometric direct volume coherence by polarimetric channel. RMS wheat ear displacements are zero (top 3 curves), 0.7cm (middle 3) and 1.3cm (lower 3). VV returns come predominantly from the top of the canopy where displacements are greatest.

coherence is preserved: sufficiently well perhaps for PolInSAR techniques to be applied. We examine the effects of clutter motion on the recovery of canopy height using PolInSAR in Fig. 5. Since we observe that HV returns are dominated by the ground-volume response, and VV returns from the direct-volume response at the top of the canopy, we examine VV and HV coherence in the complex plane for these two channels both in the absence and in the presence of clutter motion in Fig 5. Whilst for different canopies and under different circumstances this choice of channels may change, the general conclusions concerning loss of coherence in volume returns will still be applicable.

We observe a number of consequences of the effects of inter-aperture clutter motion. Firstly volume coherence is reduced. Ground-volume coherence (which dominates the HV returns) is mostly unaffected, aside from a change in underlying ground phase. The overall effect is to reduce the length of the observable coherence line and thus increase the potential error in the recovered height.

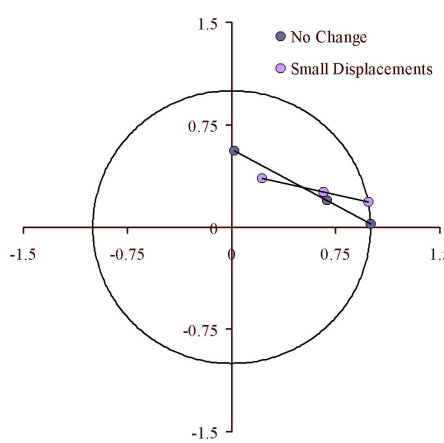

Figure 5. Effects of clutter motion on attempts to recover vegetation height and extinction using VV and HV coherence as volume and ground indicators respectively. Clutter motion shortens the extent of the sample in the complex coherence plane, and alters the recovered heights and extinctions.

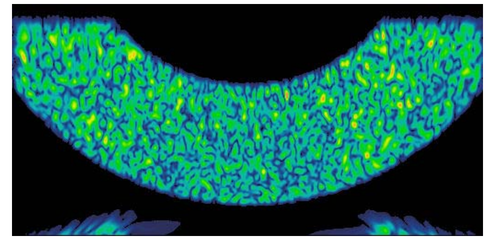

Fig. 6. Simulated static-case GB-SAR image using the distributed point scatterer model, for the parameters described in the preceding text. The image represents an area 20m in azimuth and 10m in ground-range. The features at the bottom corners are associated with range-ambiguity aliasing.

The change in coherence as a result of plant-element displacements results in different estimates of ground-phase corrected volume coherence. For this example the estimated ground-phase corrected volume-coherence changes from $\hat{\gamma}_{est} e^{-i\phi} = 0.032 + i0.56$ to $\hat{\gamma}_{est} e^{-i\phi} = 0.28 + i0.31$ in the presence of inter-aperture displacement. Since this value is related directly to canopy height and extinction estimates [9] we conclude that displacement of plant elements between SAR apertures will corrupt estimates of canopy height and extinction using polarimetric SAR interferometry.

III. Signal Processing GB-SAR Image Simulation

A. Distributed Scatterer Model

In addition to a full, physics-based calculation, we have performed signal-processing simulations with a simplified model of the vegetation target. This model consists of a distribution of point scatterers on a horizontal plane and does not provide polarimetric information. However, with this model it is possible to simulate in greater detail the swept-frequency technique used to generate GB-SAR imagery [2]. A wind force acting on the target is resolved into components parallel to and perpendicular to the principal imaging axes, so that two independent differential equations are solved at each time instant, providing exact target positional and velocity information in each of the two axes directions. Values of the mechanical constants determining the harmonic motion have been selected to be accordance with field observations. This allows the independent motions of each scatterer to be tracked during the formation of the aperture, both during the frequency sweep and from sample point to sample point along the aperture. For computational efficiency the target elements are contained within an arc over a constant inclination angle range, as motion produces spreading of the impulse response function principally in the azimuthal direction at constant inclination angle. Fig. 6 shows the static C-Band observation from a 10m height and ground-range 4m to 14m.

B. Effects of Intra-Aperture Displacement Upon Coherence

We have simulated a static image, and two images with clutter motion present, representing ‘small’ and ‘large’ RMS displacements. The small motion corresponds to a mean radial phase displacement of 0.124cm measured over all frequencies during the imaging process, as seen from the antennas point of view, and 0.375cm for the large motion.

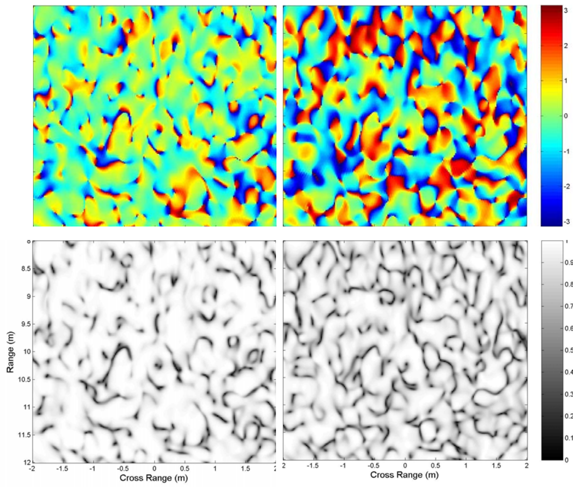

Figure 7. The top images show the phase stability ±π between the static and moving cases for mean displacements (left) 0.124cm and (right) 0.375cm , respectively, for a 4m x 4m area centered at a range of 10m. The lower images are the respective coherence images, using a sliding 5 x 5 window, and displayed over a range 0-1.

All the simulations were made with identical imaging geometries (zero interferometric baseline), and the results provide understanding of the variation of coherence with differing clutter motion. Calculations have been performed on the phase stability and corresponding coherence between the static and moving images for 4m x 4m sections of imagery centered at a range of 10m at boresight, shown in Fig. 7.

Coherence estimates are obtained using a sliding 5 x 5 pixel window, such that each pixel is not an independent measure of coherence. The derived coherence distributions are dissimilar in shape from those typically associated with interferometry. Coherence remains high at 0.9 for the small RMS displacement case, and falls to 0.81 for the large displacements. Coupled to the previous result we anticipate that small amounts of clutter motion, although having an adverse affect upon intra-aperture coherence, would not preclude the use of GB-SAR for studies in polarimetric SAR interferometry.

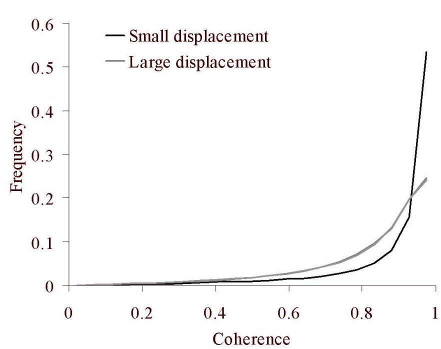

Figure 8. Coherence distributions for the motion cases discussed in the text.

IV. Conclusions

We have developed two models, a physics-based model and a signal processing model, for GB-SAR observations of wheat. The models indicate that clutter motion will degrade interferometric performance both during aperture formation, and between repeat-pass observation. However we conclude that the GB-SAR system will be robust to small amounts of clutter motion and will serve as a suitable tool for PolInSAR experimental studies.

Acknowledgment

This work has been supported by the University of Cranfield, and the Defence Science and Technology Organisation of Australia.

References

[1] S. R. Cloude and K. P. Papathanassiou, "Polarimetric SAR interferometry," *IEEE Trans. Geosci. Remote Sensing* vol. 36, p1551-1565, 1998.

[2] K. Morrison*, et al.*, "Polarimetric Calibration Strategy for Long-Duration Imaging with a Ground-Based SAR", *Canadian Journal of Remote Sensing*, vol. 31. 2005.

[3] M L Williams and S R Cloude, "Predictions of SAR Polarimetry and InSAR Coherence for a Model Wheat Canopy", *Proceedings of IEEE International Geoscience and Remote Sensing Symposium* (IGARSS 2005), Seoul, Korea, July 25-29, 2005.

[4] F. Mattia *et al.*, "Multi-Temporal C-Band Radar Measurements on Wheat Fields", *IEEE Transactions on Geoscience and Remote Sensing*, vol. 41, No.7, pp.1551-1560, 2003.

[5] P. Ferrazzoli *et al*., "Multifrequency Emission of Wheat : Modeling and Applications", *IEEE Transactions on Geoscience and Remote Sensing*, vol. 38, No. 6, pp.2598-2607, 2000.

[6] G. Cookmartin *et al*., "Modeling Microwave Interactions with Crops and Comparison with ERS-2 SAR Observations", *IEEE Transactions on Geoscience and Remote Sensing*, vol. 38, No. 2, pp. 658-670, 2000.

[7] F. Del Frate *et al*., "Wheat Cycle Monitoring using Radar Data and a Neural Network Trained by a Model", *IEEE Transactions on Geoscience and Remote Sensing*, vol. 42, No.1, pp.35-44, 2004.

[8] M Preiss and N Stacy, "Scene Coherency at X-Band from Repeat-Pass Polarimetric Interferometry", *Proceedings of IEEE International Geoscience and Remote Sensing Symposium* (IGARSS 2005), Seoul, Korea, July 25-29, 2005

[9] S. R. Cloude and K. P. Papathanassiou, "A 3-Stage Inversion Process for Polarimetric SAR Interferometry", *Radar, Sonar and Navigation, IEE Proceedings*, Vol. 150, Issue 3, pp125–134, 2003.